ELSEVIER

Brain Research Bulletin 70 (2006) 322–336

BRAIN RESEARCH BULLETIN

www.elsevier.com/locate/brainresbull

# The prefrontal cortex in the Göttingen minipig brain defined by neural projection criteria and cytoarchitecture

Jacob Jelsing [a,*], Anders Hay-Schmidt [b], Tim Dyrby [c], Ralf Hemmingsen [d], Harry B.M. Uylings [e,f], Bente Pakkenberg [a]

[a] *Research Laboratory for Stereology and Neuroscience, Copenhagen University Hospital, Bispebjerg, Bispebjerg Bakke 23, 2400-Copenhagen, Denmark*
[b] *Department of Medical Anatomy, The Panum Institute, University of Copenhagen, Copenhagen, Denmark*
[c] *Danish Research Centre for Magnetic Resonance, Copenhagen University Hospital, Hvidovre, Denmark*
[d] *Department of Psychiatry, Copenhagen University Hospital, Bispebjerg, Copenhagen, Denmark*
[e] *Netherlands Institute for Neuroscience, KNAW Amsterdam, The Netherlands*
[f] *Department of Anatomy, VU University Medical Center, Amsterdam, The Netherlands*

Received 31 January 2006; received in revised form 24 April 2006; accepted 11 June 2006
Available online 5 July 2006

**Abstract**

In an attempt to delineate the prefrontal cortex (PFC) in the Göttingen minipig brain the distribution of reciprocal thalamocortical projections was investigated using anterograde and retrograde tracing techniques and evaluated in relation to the specific cytoarchitectonic organization. Tracers were visualized using standard immunohistochemistry or evaluated in vivo using manganese ($Mn^{2+}$) as an MRI paramagnetic tracer. The in vivo tract tracing turned out to be very sensitive with a high correspondence to the histological labelling. Tracers injected into the mediodorsal thalamus labelled the medial and rostral pole of the frontal lobe as well as the anterior cingulate, anterior insular and dorsomedial frontal cortices. Subsequently, the reciprocity and specificity of these connections were tested from injections into the traced frontal cortices indicating that the PFC has cortical connections to different parts of the MD nucleus. Although the granular layer IV, characteristic of primate PFC could not be identified, both cytoarchitectonic and connectional data suggests that the Göttingen minipig has a structurally divided prefrontal cortex. Stereological estimates of PFC volume showed that the Göttingen minipig PFC constitutes about 24% of the total neocortex volume and 10% of the total brain volume.


*Keywords:* Cytoarchitecture; Manganese; MRI; Neuron tracing; Stereology; Volume

## 1. Introduction

Being one of the most evolved brain regions involved in human cognition and behaviour the prefrontal cortex (PFC) is considered an area of primary interest for a number of neurological and psychiatric disorders including schizophrenia and dementia (e.g. [26]). Based upon the cytoarchitectonic criterion of having a granular layer IV and a location rostral to the agranular premotor areas, the PFC was considered unique to the primate species [8,9] until Rose and Woolsey [53] re-defined the PFC as the cortical projection area of the thalamic mediodorsal (MD) nucleus. However, with the advent of more refined tracing techniques it has become apparent that the PFC also con-

*Abbreviations:* an, ansate sulcus; AC, anterior cingulate cortex; AId, dorsal anterior insular cortex; AIm, medial anterior insular cortex; AIv, ventral anterior insular cortex; CM, centromedian nucleus; cin, cingulate sulcus; cor, coronal sulcus; cru, cruciate sulcus; dFr, dorsofrontal region; dlFr, dorsolateral frontal cortex; dmFr, dorsomedial frontal cortex; Il, infralimbic cortex; LD, lateral dorsal nucleus; M1, primary motor cortex; MD, mediodorsal nucleus of the thalamus; MDc, central part of MD; MDl, lateral part of MD; MDm, medial part of MD; mpFr, mediopolar frontal cortex; mpFrl, lateral mediopolar frontal cortex; PC, posterior cingulate cortex; PI, posterior insular cortex; PrM, premotor cortex; R, reticular nucleus of the thalamus; prs, presylvii sulcus; SC, somatosensory cortex; sig, sigmoid gyrus; spl, splenial sulcus; sup, superior frontal gyrus; syl, sylvii sulcus; VL, ventral lateral nucleus of the thalamus; VP, ventral posterior nucleus of the thalamus

* Corresponding author. Tel.: +45 3531 6425; fax: +45 3531 6434.
*E-mail address:* jje@rheoscience.com (J. Jelsing).

0361-9230/$ – see front matter © 2006 Elsevier Inc. All rights reserved.
doi:10.1016/j.brainresbull.2006.06.009

nects to other thalamic nuclei and that thalamic MD projections appear to reach some cortical areas outside the prefrontal cortex [27,30,63,64]. As a consequence the debate about the nature and characteristics of the PFC in non-primate species has resumed [49,62].

Considering the dimensions of the gyrencephalic pig brain, which is comparable to that of humans in gross anatomy, growth and development (e.g. [18,22]), we believe pigs may potentially prove useful as an animal model of human frontal lobe function or dysfunction. However, there are practically no data available regarding the localisation of the PFC in the pig brain. Stephan [59] describes and delineates a dysgranular frontal cortical area, which he believed to correspond to Brodmann's area 8, and a corresponding region is briefly described as prefrontal by Campbell [11]. Weaver et al. [68] dissects the prefrontal cortex from pigs without mentioning on what anatomical basis the definition was made, and Fang et al. [21] considers the mediofrontal cortex as prefrontal. To the author's knowledge, no neural-tract tracing has previously been performed concerning reciprocal thalamocortical connections in the pig brain.

A number of anatomical and functional criteria should optimally be considered to evaluate whether pigs have a prefrontal cortex. This includes the pattern and density of specific connections, functional properties, the presence and distribution of specific neuroactive substances and neurotransmitter receptors, the embryological development and for closely related species, the cytoarchitectonic characteristics [12]. For the initial purposes of the present study the PFC was defined as the major reciprocal projection area from the MD nucleus, the key definition according to Uylings and van Eden [63]. Specifically, neuronal tracers were used to study the reciprocal projection patterns from the MD nucleus to regions of the frontal cortex providing a baseline for corresponding injections into the labelled frontal cortical regions. Only those frontal cortical regions for which the reciprocal connections with the MD were strong in terms of a relative high number of both projecting neurons and terminals, were included in the definition of the PFC. The cytoarchitectonic characteristics of the frontal regions are described to correlate the tracer data.

## 2. Materials and methods

### 2.1. Animals

A total of 17 young Göttingen minipigs were used in the study (12 males and 5 females, 3 months of age, mean weight 5.5 kg, coefficient of variation (CV) = 0.17). All surgical procedures were carried out according to guidelines for the care and use of animals approved by the Danish Animal Experiments Inspectorate.

### 2.2. Procedure

#### 2.2.1. Surgery

Pigs were anesthetized with an intramuscular injection (1 ml/10 kg bodyweight) of a mixture of 6.5 ml Narcoxyl® Vet (20 mg/ml), 1.5 ml Ketaminol® Vet (100 mg/ml) and 2.5 ml Methadone DAK (19 mg/ml) added to one bottle of Zoletil®50 Vet without additional solvent. The pigs were intubated using an endotracheal tube, Rüsch size 4.0 mm i.d. and placed in the stereotaxic instrument (see below). Post-operatively, the pigs received a 0.5 ml i.m. injection with Rimadyl® (50 mg/ml), 0.5 ml Streptocyllin® (250 mg/ml) followed by 0.2 ml Temgesic® (0.3 mg/ml). The pigs were supplied with an additional injection of Temgesic® 8 h later.

#### 2.2.2. Tracer Injection

A monkey Kopf stereotaxic instrument was adapted for the pig brain to permit fixation of the skull by ear-bar supports and a mouthpiece. The stereotaxic zero point was defined as the external skull structure, bregma, using the upper margin of the infraorbital ridge and the upper margin of the external auditory meatus as a horizontal zero plane [54]. Six pigs received injections directed towards the MD nucleus (using the stereotaxic coordinates: anterior +2.5 mm; horizontal −30.0 mm; and lateral ±2.5 mm), and 11 pigs received injections in frontal cortical areas (Table 1). The latter injection sites were selected as areas of primary interest based on the anterograde- and retrograde tracings from injections in the MD nucleus. All animals received a bilateral injection of two different histological tracers, biotinylated dextran amine (BDA, 10,000 molecular weight, Molecular Probes, Eugene, OR) and Cholera toxin-subunit B (ChB, List Biological Laboratories, Campbell, CA) except for five animals receiving a simultaneous injection of BDA and $MnCl_2$ (Sigma-Aldrich, Denmark). BDA (10% (v/v) in 0.15 M phosphate-buffered saline, pH 7.4 (PBS)) and $MnCl_2$ (0.8 M $MnCl_2$ Tetrahydrate) were used for anterograde labelling, and ChB (1% (v/v) in PBS) for retrograde labelling. Tracers were delivered singly or simultaneously by pressure injection (gently by hand) through Hamilton syringes fitted with 26 G and 22 G needles.

#### 2.2.3. MRI data collection and analysis

To study cortical efferents to the MD nucleus in vivo five pigs received a simultaneous injection of the anterograde tracers manganese ($MnCl_2$, 0.8 M in physiological saline water) and BDA (Table 1). Two of these pigs received a bilateral injection and three pigs received a unilateral injection. The anaesthetized pigs were transported to the MR scanner, placed in a prone position and fixed in an eight channel head coil. Maintenance of anesthesia was accomplished by an i.m. injection of 0.2 ml Zoletil (mixture as described above) every 20 min. The MR-scanning was performed using a Magnetom Trio (3 T) imager (Siemens Medical Systems). Structural images were acquired using a T1-weighted magnetization prepared gradient echo (MPRAGE) sequence, which is sensitive to the paramagnetic tracer, manganese. Sequence parameters were: TR = 1580 ms, TE = 3.93 ms, TI = 800 ms, flip angle = 9°, slice thickness = 0.6 mm, image matrix: 256 × 256, FOV = 160 mm × 160 mm and voxel size: 0.6 mm × 0.6 mm × 0.6 mm. In addition to a baseline MRI acquisition, in vivo anatomical acquisitions were obtained at Days 2 and 4 after injection. To increase signal-to-noise ratio each acquisition was repeated 8, 16 and 15 times for baseline, Day 2 and Day 4, respectively.

Prior to analysis, the acquired MR data for each pig was processed in the following manner: stripping of the brain from non-brain [43], co-registration to the first baseline image using 6 degree-of-freedom [58] and finally re-sliced with a B-spline interpolation [58].

A voxel wise *T*-test (Student's *t*-test) with Bonferroni correction was finally performed between the baseline and the joint of the two acquisitions following injection.

#### 2.2.4. Histology and tissue processing

Following a 7–14 days survival period, the animals were premedicated with 0.5 ml of Zoletil (mixture as described above) and placed in a supine position on the operation table. Just before intervention the pig was supplied with a lethal dose of 5.0 ml Pentobarbital i.v. The deeply "anesthetized" pig then received a midsternal incision followed by a sternal split. The left cardiac ventricle was punctured by an infusion cannula (3-mm outer diameter), the right auricle was cut open and a transcardial perfusion with 0.5 l saline followed by 2.5 l of 4% paraformaldehyde (PFA) in PBS was executed. The procedure took on average 10–15 min.

Following perfusion the brain was removed and postfixed for 24 h in 1% PFA at 5 °C, transferred to 30% sucrose in PBS for 2 or 3 days at 5 °C, frozen on dry ice and cut coronally into a series of 100 μm thick cryosections on a Olympus Ultrapro 5000 cryostat. Every third section was collected and stored in cryoprotectant at −20 °C until reacted. Both tracers were visualized in the same sections in sequential fashion: BDA first and ChB second. Additional

Table 1
Frontal injections and corresponding projections sites based tracing studies on 11 minipigs. As a result of large injection sites and diffusing tracer, tracer uptake in adjoining areas (shown in parentheses) should be considered. LH = left hemisphere; RH = right hemisphere; UT = unsuccessfull tracing. For other abbreviations, see 'List of Abbreviations' in text

| Animal # | Tracer | Coordinates from Bregma | Injection site | Main projection site | Ref # Fig. 7 |
|---|---|---|---|---|---|
| 1_LH | 5 μl BDA | +20.0; −10.0; +2.0 | AC | MDc, MDl | 3 |
| 1_RH | 2.5 μl BDA, 2.5 μl ChB | +12.5; −10.0; −2.5 | PrM | VA, VL | 9 |
| 2_LH | 2.5 μl BDA, 2.5 μl ChB | +25.0; −15.0; +2.0 | mpFr | MDm | 4 |
| 2_RH | 5 μl ChB | +15.0; −15.0; −2.5 | Aimed for Il | *UT* | |
| 3_LH | 2.5 μl BDA, 2.5 μl ChB | +25.0; −15.0; +4.0 | mpFrl (AIv) | MDm, MDc, CM | 5 |
| 3_RH | 2.5 μl BDA, 2.5 μl ChB | +10.0; −20.0; −2.0 | Aimed for Il | *UT* | |
| 4_LH | 2.5 μl BDA, 2.5 μl ChB | +25.0; −10.0; +4.0 | mpFrl (Aid, dlFr) | MDm, MDc, CM, VA | 6 |
| 4_RH | 5 μl BDA | +12.5; −10.0; −2.0 | dmFr (PrM, ACd) | MDc, MDl | 10 |
| 5_LH | 0.5 μl BDA, 0.5 μl ChB | +15; −10.0; +2.5 | AC | MDc, MDl | 11 |
| 5_RH | 0.5 μl ChB | +7.5; −15.0; −15.0 | Aimed for AIm | *UT* | |
| 6_LH | 0.5 μl BDA, 0.5 μl ChB | +7.5; −15.0; +2.0 | AC (PrM) | MDl | 14 |
| 6_RH | 0.5 μl BDA | +7.5; −20.0; −15.0 | Aimed for AIv | *UT* | |
| 7_LH | 1 μl BDA, 1 μl $MnCl_2$ | +20.0; −7.5; +2.0 | dmFr | MDc | 2 |
| 7_RH | 1 μl BDA, 1 μl $MnCl_2$ | +10.0; −10.0; −2.0 | PrM (dmFr) | VA, MDl | 12 |
| 8_LH | 4 μl BDA, 1 μl $MnCl_2$ | +20.0; −10.0; +7.0 | SC | VL, VLP | 7 |
| 8_RH | 4 μl BDA, 1 μl $MnCl_2$ | +7.5; −15.0; −2.0 | Aimed for caudal AC | *UT* | |
| 9_RH | 4 μl BDA, 1 μl $MnCl_2$ | +27.0; −15.0; −2.5 | mpFr | MDm | 1 |
| 10_RH | 4 μl BDA, 1 μl $MnCl_2$ | +10.0; −10.0; −2.0 | PrM (AC) | VA, VL, MDl | 13 |
| 11_LH | 4 μl BDA, 1 μl $MnCl_2$ | +20.0; −12.5; +2.0 | AC | MDc | 8 |

sections were visualized separately for BDA and ChB or counter stained with thionine for histological delineations. Prior to all staining procedures the free-floating cryosections were rinsed in several shifts of Tris buffered saline (TBS) (0.05 M Trizma base, 0.15 M NaCl, pH 7.4) to wash out all sucrose and glycerol from the cryoprotectant. Endogenous peroxidase activity was blocked by incubation for 30 min in 1.5% $H_2O_2$ in methanol. Sections were rinsed 3× 15 min in TBS + 1% Triton X-100, incubated for 60 min in a 10% (v/v) fetal bovine serum (FBS) in TBS and incubated in primary goat anti-ChB antiserum (List Biological Laboratories, Campbell, CA) diluted 1:4000 overnight at 5 °C under gentle agitation. The following day, sections were washed in TBS + 1% Triton X-100 for 3× 15 min, incubated in streptavidin–biotin–HRP complex (DakoCytomation, Denmark) diluted 1:200 in TBS + FBS for 90 min, rinsed in TBS 3× 15 min before the HRP-labelled BDA was visualised in a TBS staining solution containing 0.5 mg/ml diaminobenzidine (DAB) added 0.2 μl/ml $H_2O_2$ for 10–15 min resulting in a brown reaction product. Sections were then rinsed 1× 5 min in PBS, blocked in 1.5% $H_2O_2$ in TBS for 15 min and washed 3× 15 min in TBS + 1% Triton X-100, followed by incubation at room temperature in biotinylated donkey anti-goat IgG $(Fab)_2$ antibody diluted 1:2000 (Jackson Immunoresearch Lab., West Grove, PA) for 90 min. After rinsing 3× 15 min in TBS + 1% Triton X-100, sections were incubated in HRP–streptavidin diluted 1:200 in TBS + FBS for 90 min, rinsed in TBS 3× 15 min before HRP-labelling of the secondary ChB biotinylated anti-goat IgG was visualised in VIP or SG (both Vector Laboratories) resulting in a dense violet or blue/black reaction product. Finally, the sections were rinsed 3× 15 min in Tris buffer, mounted on 3% chromalum/gelatine coated slides, dried for at least 2 h, dehydrated and cover slipped. Single-antigen immunohistochemistry were routinely processed for control sections by either omitting the ChB primary antigen or using a HRP anti-goat IgG diluted 1:2000 (Jackson Immunoresearch Lab., West Grove, PA).

One series of sections from each pig was counterstained by thionine for cytoarchitectonic delineations. Prior to thionine staining, sections were defattened in 2× 30 min shifts in 100% acetone, 1× 15 min in 96% acetone and 1× 15 min in 70% acetone.

### 2.3. Method of analysis

Cytoarchitectonic and tracing analyses were performed using a compound microscope (Olympus BX50) mounted with a Color View I (3.3 MegaPixel CCD Camera). To obtain final images as true to the microscopic view as possible, and to achieve optimal presentation, the digitally acquired images were reoriented and/or adjusted for brightness, contrast, or color balance in photoimaging software (Adobe Photoshop). Graphic illustrations were performed on transposed sections using Adobe Illustrator.

Stereological volumes were obtained applying the Cavalieri theorem of systematic sampling in combination with point-counting [33]. A 2D systematic point grid was superimposed uniformly randomly onto a systematic randomly pre-selected number of thionine stained sections. Points hitting the structure of interest, i.e. the delineated PFC, the neocortex and the total brain were converted into volumes using the formula:

$$V(\text{ref}) = k\bar{t}a(p)\sum P$$

where $k$ is the inverse sampling fraction, $\bar{t}$ the average section thickness, $a(p)$ the area associated with each point of the grid and $\sum P$ is the total number of points hitting the region of interest.

## 3. Results

To introduce readers to the specific terminology, cytoarchitectonic characteristics for the cortical and thalamic regions will be presented first.

### 3.1. Cytoarchitectonic analyses

Even though a number of cytoarchitectonic subdivisions are clearly distinguishable within the frontal cortex of the pig brain, the structure and cellular organization of the frontal cortex in the young Göttingen minipig brain, or the pig brain in general, has not previously been analyzed in detail. There exist two rather comprehensive cytoarchitectonic cortical maps of the pig brain neocortex [11,59] in addition to a number of studies on specific cortical regions [37,48]. However, the conclusions and homology assessments are rather inconsistent and supplementary analyses are considered of essential value. This also accounts for the assessment of sulci and gyri patterns, especially related to the mediofrontal and central sulci (e.g. [15,16,59]). In

the present study we have used the terminology used recently by Okada et al. [44].

*3.1.1. Subdivisions of the frontal cortex*

A cytoarchitectonic analysis was performed in an attempt to differentiate the observed projection areas in the frontal cortex into anatomical borders of the young Göttingen minipig PFC. Based on the examination of thionin stained coronal sections it was evident that the frontal cortex rostral to the central ansate sulcus of the young Göttingen minipig could be divided into several cytoarchitectonically defined cortical areas. The PFC is here separate into four principal regions; the frontopolar, the anterior cingulate, the anterior insular and the dorsofrontal region (Fig. 1). All these areas lack a granular layer IV.

*3.1.1.1. The frontopolar region.* The mediopolar frontal (mpFr) (Figs. 1 and 2) covers the rostral tip and ventral aspect of the frontal pole as well as parts of the medial surface. Laterally, it expands in the wall of the praesylvii and rhinal sulcus rostral to the union of the frontal pole with the olfactory bulbus (Fig. 1). Medially, it is surrounded by the dorsomedial frontal area and the anterior cingulate cortex (see below). As in all other frontal areas mpFr is essentially agranular, thus lack a granular layer IV. The most characteristic feature of the mpFr is the two dark bands in the infragranular layers V and VI being separated by a relative cell poor zone layer Vb. In general, the dark band in layer VI has a higher cellular density than observed in any other cortical areas (Fig. 2). Layer III has two sublayers with a higher cellular density in the upper layer IIIa, than in the lighter IIIb.

The mpFr is relatively homogeneous, and may be considered as a single area. However, related to certain variations in the structural organization especially in the infragranular layers, we delineated a lateral (mpFrl) subdivision as well (not shown). In the mpFrl, the dark band in layer VI is smaller than in the remainder of the mpFr, with more clear and larger cell somata.

*3.1.1.2. The anterior cingulate cortex.* The anterior cingulate (AC) (Figs. 1–3) is found around the genu of the corpus callosum. It is here subdivided into an inner caudal area and a rostrodorsal area. A cingulate subcallosal area is also observed.

AC is characterized by large, oval and clear cell somata in layer III and layer VI. The inner caudal area (Fig. 2) is distinguished from the rostrodorsal area (not shown) by an increased density in layer V cells, which is organized in two distinct sublayers Va, Vb (Fig. 2). Further subdivisions of the AC can be identified but they are not described separately. Nor are the periallocortical area and the induseum griseum observed as thin cortical strips dorsal to the genu of the corpus callosum containing three to four layers.

The subcallosal or infralimbic (IL) area (Fig. 3) is located ventral to the genu of the corpus callosum and is for now considered to be a part of the anterior cingulate cortex. It is delimited caudally by the septal nuclei and is easily recognized by a layer II which contains clusters of cells separated by vertical cell poor strips of fibre bundles.

The posterior cingulate (PC) is located in between the callosal and splenial sulcus (Fig. 3). The PC is not considered to be a part of the Göttingen minipig PFC (see below). In contrast to AC, the most characteristic feature of the PC is the separation of layer III

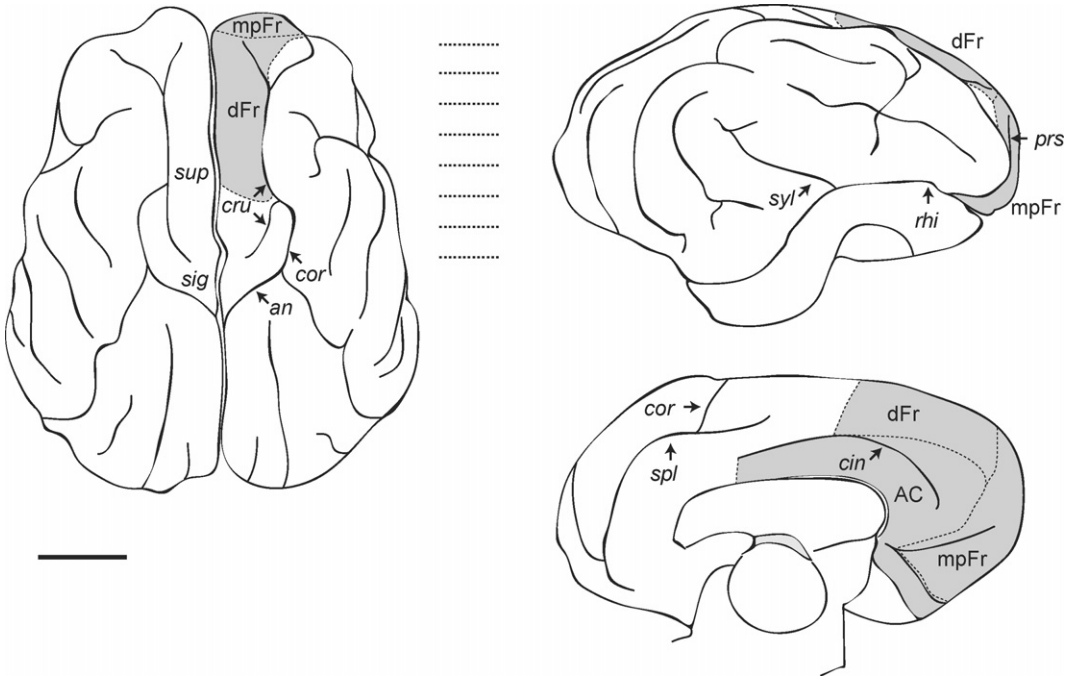


Fig. 1. Schematic illustration of the young Göttingen minipig brain seen in dorsal, lateral and medial view. The PFC cortex (grey area) occupies the rostral part of the superior frontal gyrus, a large frontomedial area including anterior cingulate as well as the anterior insula buried within the deep rhinal sulcus (concealed from external view). The four major regions are tentatively outlined with stippled lines. Horizontal lines indicate approximate position of sections shown in Figs. 2, 3, 6 and 7. For abbreviations, see 'List of Abbreviations' in text. Scale bar = 1 cm.

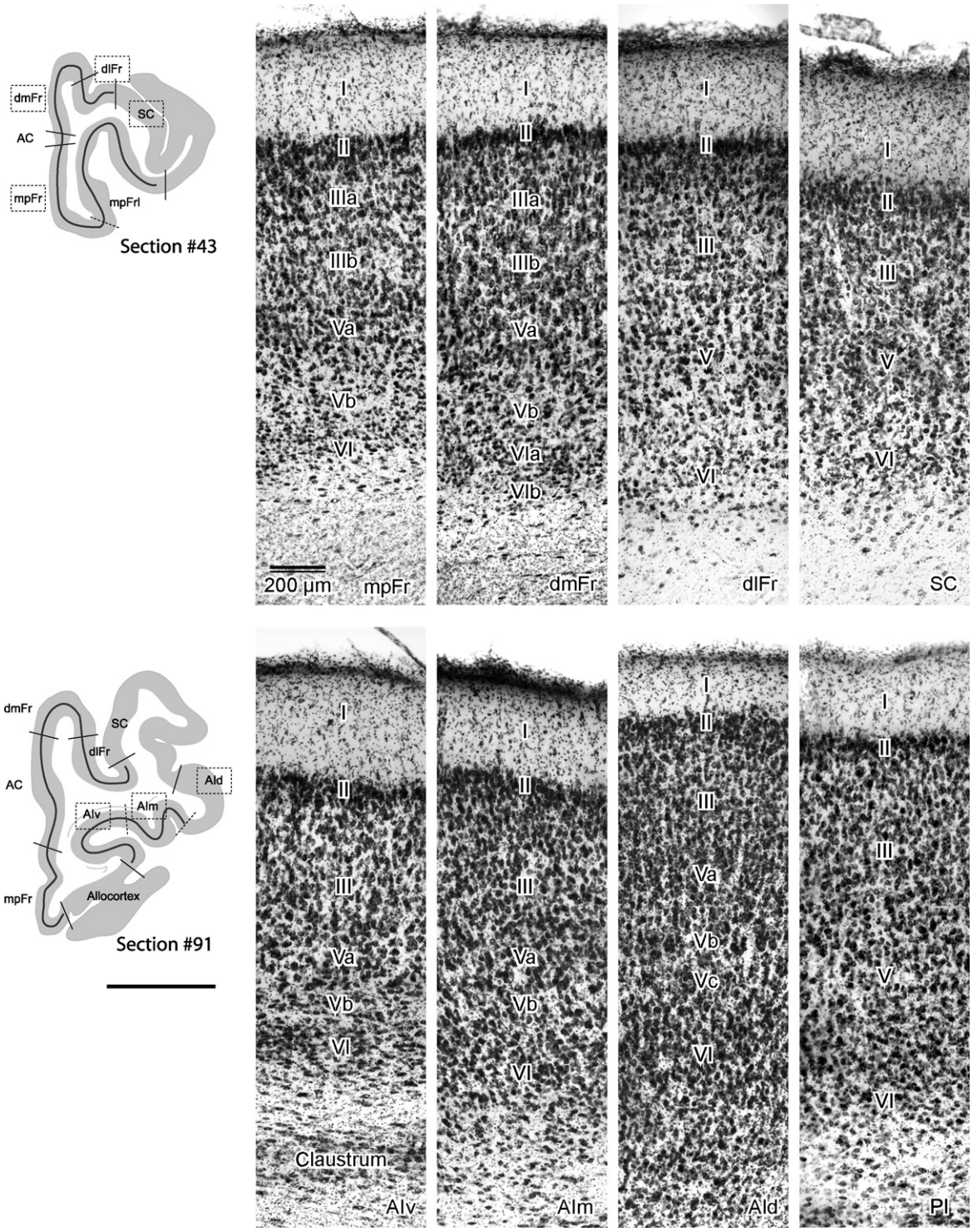


Fig. 2. Cytoarchitectonic delineations of the rostrofrontal cortices of the Göttingen minipig brain. Coronal section plane. Full line indicates PFC areas. For abbreviations, see 'List of Abbreviations' in text. Scale bar = 1 cm.

from layer V by a granular layer IV. Layer III appears relatively smaller in PC and layer V is subdivided into two sublayers; layer Va, with larger cell somata, and a smaller, less cell dense and light layer Vb.

*3.1.1.3. The anterior insular cortex.* The anterior insula occupies the cortex along the claustrum and the rhinal sulcus (Figs. 1–3). More caudally, it borders the posterior insula. The anterior insula is subdivided into three divisions; ventral insular, medial insular and dorsal insular.

The ventral anterior insular (AIv) (Fig. 2) occupies the ventral bank of the rhinal sulcus bordered ventrally by the allocortex and by the medial insular above it. It has a comparatively low cellular density in layer III and a low frequency of large layer V cells

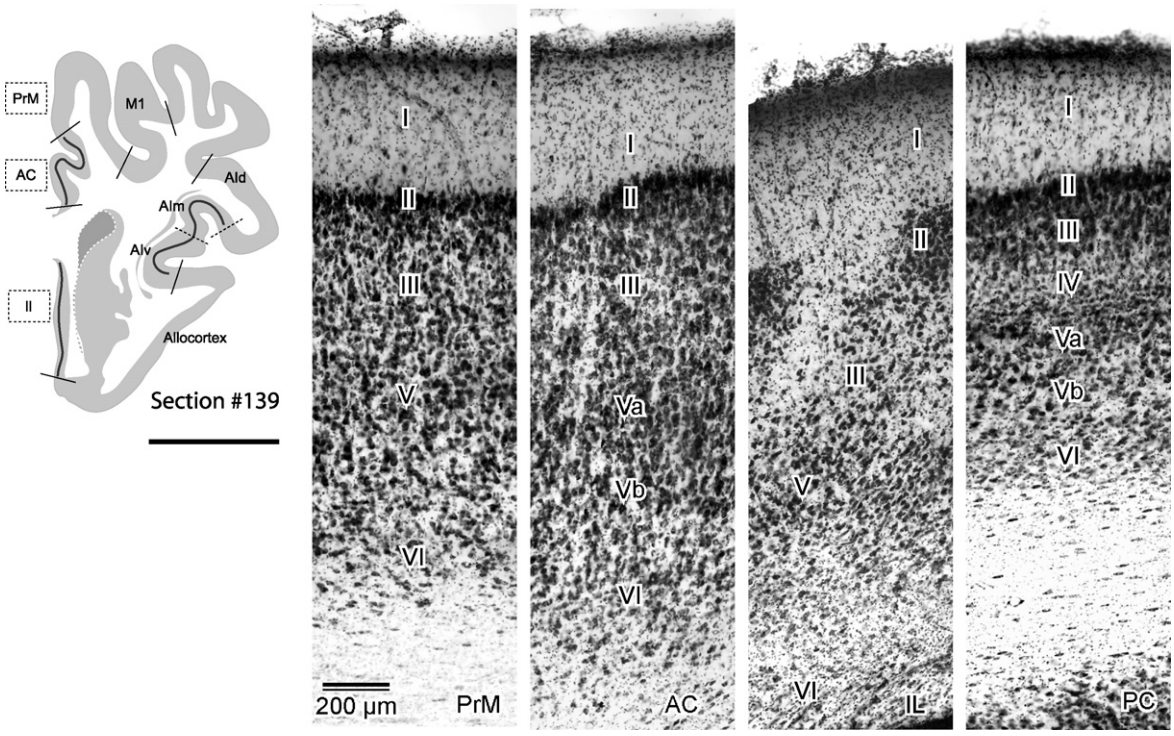


Fig. 3. Cytoarchitectonic delineations of the caudofrontal cortices of the Göttingen minipig brain, coronal section plane. Full line indicates PFC areas. For abbreviations, see 'List of Abbreviations' in text. Scale bar = 1 cm.

compared to AIm and AId. At low magnification layer VI looks light with a cell sparse layer Vb intercalated between layer V and VI.

The medial anterior insular (AIm) (Fig. 2) occupies the dorsal bank of the rhinal sulcus. A somewhat higher cell density in layer III, a sublayer Vb with large somata and the absence of a light zone between layer V and VI characterizes the AIm. The absences of a light zone in the infragranular layers gives layer VI a more dense appearance.

The dorsal anterior insular (AId) (Fig. 2) is the only part of the anterior insular which is not hidden within the rhinal sulcus. It is considerable thicker than the ventral and medial insular with a high density of small layer III cells. The largest differences compared to AIv and AIm are noticeable in layer V and VI. Layer V are organized in radial rows with a small, nearly one cell thick layer Vb with large somata followed by a light zone and a cell poor layer Vc. Layer VI is wide and dark. The AId is not considered to be a part of the pig PFC (see below).

The posterior insular (PI) develops from the rostral extreme of the sylvii sulcus, caudal to the anterior insular (Fig. 1). The PI resembles AId, but it has no characteristic layer Vb, and the cellular density of layer III is also lower than in AId. We did not divide the PI into subareas, since it is not included in the pig PFC (see below).

*3.1.1.4. The dorsofrontal region.* The dorsofrontal region is found on the shoulder and medial/lateral aspects of the superior frontal gyrus (Figs. 1 and 2). Caudally, it borders to the premotor area. It is divided into two relatively homogeneous subregions.

The dorsomedial frontal (dmFr) (Fig. 2) is seen on the crown and dorsomedial surface of the superior frontal gyrus. Caudally it converges into the premotor cortex (PrM), with which it has some cytoarchitectonic resemblance. It is characterized by a dense appearance of layer II, a dense and homogeneous layer III with large somata in the deep sublayers, and the large densely stained pyramidal cells in the relatively wide layer Va. Layer Va is separated from the relative cell dense layer VI by a lighter layer Vb, and layer VI may be divided into an upper and lower less cell dense layer.

The dorsolateral frontal (dlFr) (Fig. 2) is observed at the lateral aspect of the superior frontal gyrus, i.e. in the fundus of the cruciate sulcus. It constitutes the dorsolateral extreme of the pig prefrontal cortex and is basically distinguished from the dmFr by the oval and less dense cells in layer VI, which is not as well separated from layer V as in dmFr.

*3.1.1.5. Adjoining cortices.* In addition to the posterior cingulate, the posterior insular and the dorsal anterior insular cortices, which have already been described, allocortex, septal nuclei, motor cortices and a lateral somatosensory region borders the Göttingen minipig PFC (Figs. 1–3).

A premotor-like cortex (Figs. 1 and 3) is observed in the superior frontal gyrus, rostral to the developing cruciate sulcus and caudal to the dorsofrontal prefrontal region. It is distinguished from dorsofrontal PFC areas by a less cell dense layer III, an increasing number of large pyramidal neurons in a wide layer V and clear, oval cells in layer VI.

A primary motor-like area (M1) (not shown) expands in the medial wall of the coronal sulcus, delimited caudally by the cen-

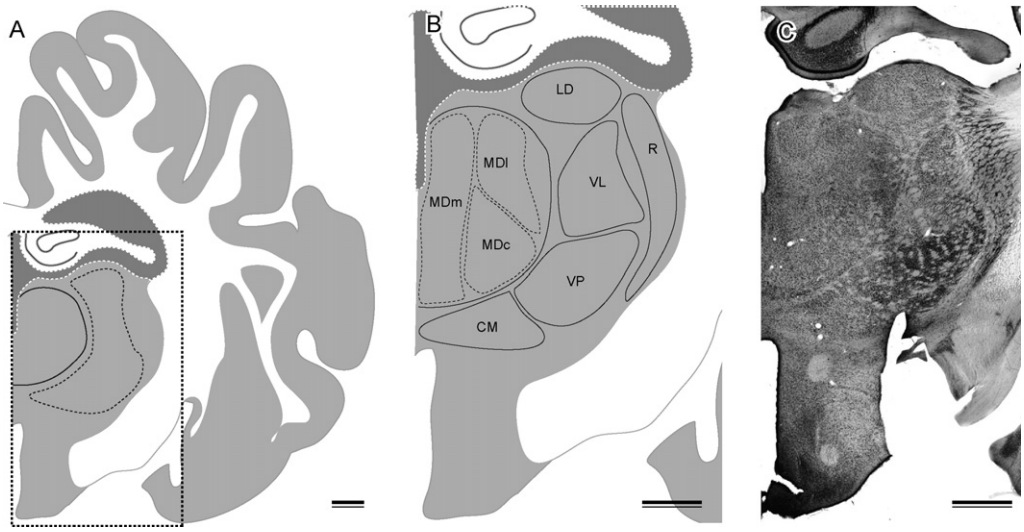


Fig. 4. Delineations of the thalamic nuclei with parcellation of the MD thalamus into medial (MDm), central (MDc) and lateral (MDl) subdivisions, coronal section plane. For abbreviations, see list. Scale bar = 2 mm.

tral ansate sulcus. A sublayering of layer III and a low density of very large, loosely dispersed cell somata in layer V characterize the M1.

A somatosensory cortex (SC) delimits the prefrontal cortex laterally, both at its ventral and dorsal extreme (Fig. 2). SC has a large frequency of large layer V cells and the infragranular layers have in general a low cellular density. Though differences in the cellular arrangement are discernible, especially at its caudal expansion, the SC bordering the PFC is here not subdivided.

#### 3.1.2. Subdivions of the MD nucleus

The thalamic nuclei were delineated in Nissl stained sections and compared to available descriptions of the thalamus in the domestic pig [22,52,57] and other mammals [35]. The MD nucleus is well developed in the Göttingen minipig and is here divided into a medial, central and lateral subregion (Fig. 4). However, boundaries are difficult to define exactly, especially at the caudal and rostral borders of the nucleus.

The medial MD (MDm) is composed of densely stained, homogeneously arranged cells. It is located at the medial aspect of the nucleus in its full rostrocaudal and dorsoventral extent.

The central MD (MDc) is located in the centroventral part of the nucleus. It is most prominent in the middle part of the MD nucleus (in the rostrocaudal extent). The cells are less densely stained than in MDc and loosely arranged in a dense neuropil.

The lateral MD (MDl) is observed in the lateral aspect of the MD nucleus where it borders the central lateral nucleus. It is most prominent in the middle and caudal extent of the MD nucleus and characterized by the high spatial density of darkly stained cells.

An even more darkly stained densocellular-like area is observed along the most dorsolateral extension. The densocellular area is by some authors allocated to the central lateral intralaminar nucleus [35].

### 3.2. Neuron tract tracing

#### 3.2.1. Thalamic injections

All injections directed towards the thalamus were positioned in the MD nucleus (Figs. 5 and 6). However, because the foci of pressure injections, as demonstrated with immunoperoxidase staining (Fig. 5(A)), were usually not limited to the intended area, projections from other neighbouring nuclei, e.g. the intralaminar or midline nuclei could unintentionally also be involved. Consequently, only a global picture of medial thalamic projections could be determined. Furthermore, two injection loci turned out to be placed rather close to the caudal part of the MD nucleus leading to a possible tracer uptake also from the posterior nuclei of the thalamus.

The global cortical distribution of anterogradely labelled terminal fields and retrogradely labelled neuronal perikarya is illustrated in Fig. 6. BDA turned out to be transported both anterogradely and retrogradely in the pig brain (Fig. 8(L)). Large areas of the frontal cortex were labelled. The strongest projections were found in the medial and rostral parts of the frontal pole (i.e. in the mpFr), but dense connections were also observed in the dorsofrontal region, the anterior cingulate and in parts of the anterior insular cortex (Fig. 6). All projections had a characteristic laminar distribution with anterogradely projecting fibres terminating in deep layer III and retrogradely labelled perikarya in layer VI (Fig. 5(B and C)).

#### 3.2.2. Frontal cortical injections

The cortical injection sites are illustrated in Fig. 7 and the principal results summarized in Table 1. Five injections aimed for either the insular cortex, the subcallosal area or the caudal extension of the cingulate cortex were misplaced in CSF or white matter (Table 1); these are not shown in Fig. 6.

In general, all successfully performed injections resulted in a dense labelling of both terminals and perikarya in the MD nucleus (Figs. 5(E, F, H), 7). Thalamic labelling was also observed in the ventral anterior and ventral lateral nucleus, usu-

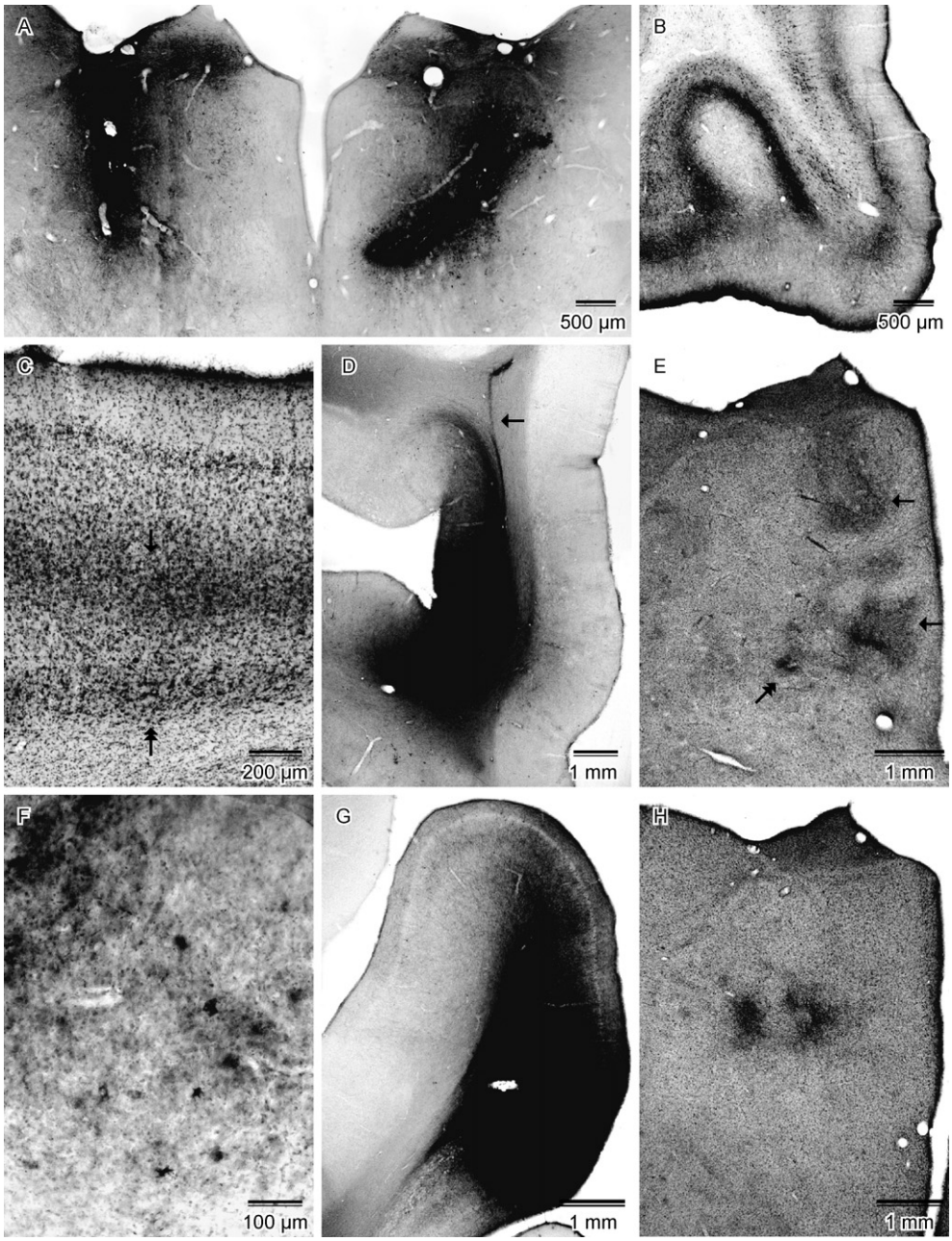


Fig. 5. Brightfield photomicrographs of tracer injection sites and projection sites. Bilateral injection of tracer into the thalamic MD nucleus (A) and the corresponding efferent and afferent connections with the frontopolar PFC (B). (C) Anterogradely labelled thalamocortical fibres terminate in deep cortical layer III (arrow) with retrogradely labelled perikarya in cortical layer VI (double arrow). Frontal injection of tracers into ventrolateral mpFr (D, Fig. 7, #5) with tracer transport in white matter (arrow) toward final termination in the medial MD nucleus (E, arrow) of both retrogradely and anterogradely labelled cell processes (F). Notice also some labelling in the central part of the MD nucleus (E, double arrow). (G) Injection in the dmFr (Fig. 7, #10), with possible tracer uptake in neighbouring areas, terminates in the central and lateral part of the MD nucleus (H).

ally as projections from areas adjacent to the premotor cortex, or in intralaminar and midline nuclei. However, these projections were not predominant. Four injections positioned in the frontal cortex appear to have a stronger reciprocal connection to other thalamic nuclei than the MD nucleus (injection no. 7, 9, 12–13 in Fig. 7, Table 1). The PrM is more strongly connected to the VA and VL, and the SC to the VL and VLP nuclei. As a consequence of the relatively large injection loci (Fig. 5(D, G)) tracers might have been taken up in neighbouring cortical areas. This has been taken into account in the evaluation of the specific tracings.

The reciprocal prefrontal corticothalamic connections appear to be topographically organized in the MD nucleus depending on the specific location of injections in the frontal cortex (Fig. 7). In the Göttingen minipig, the medial part of the MD nucleus (MDm) seems to be related to the mpFr, whereas the central part (MDc) and lateral part (MDl) is mainly connected with the anterior cingulate and the dorsofrontal region. At present,

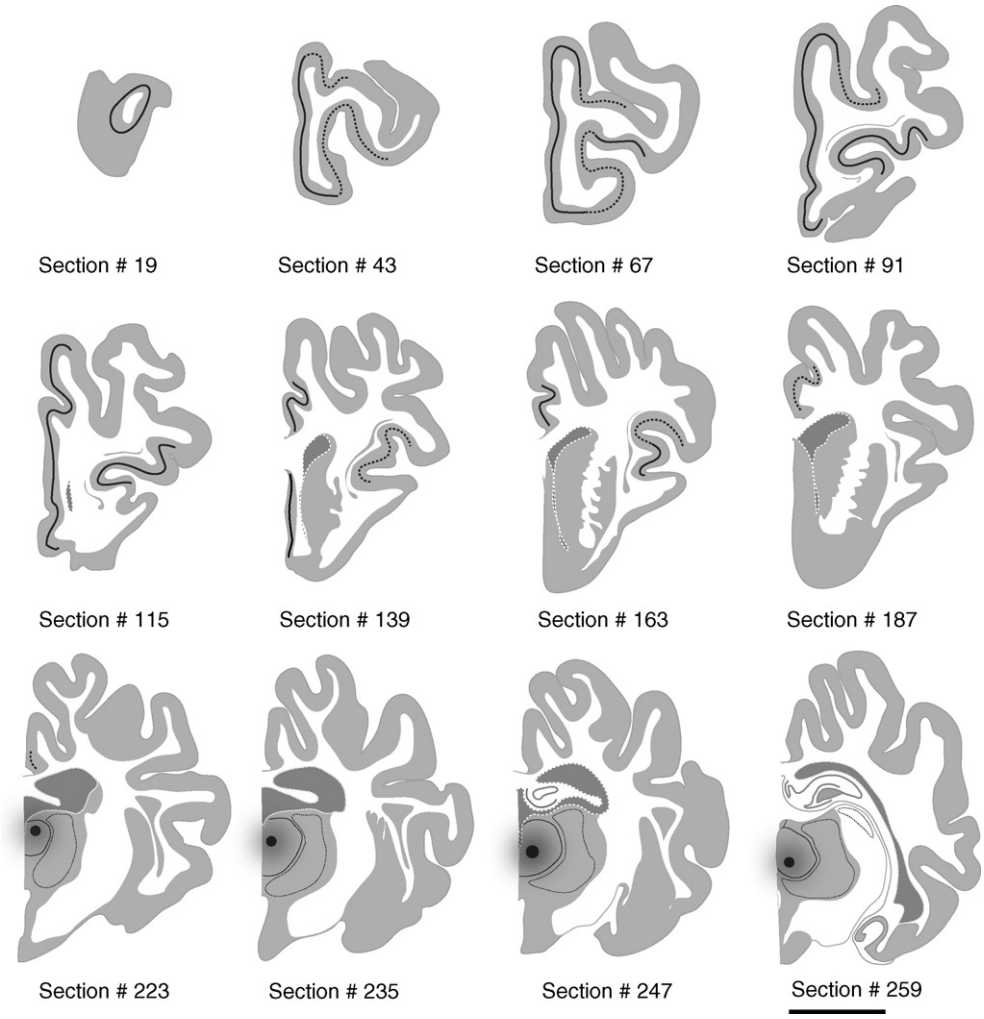


Fig. 6. Schematic illustration of coronal sections demonstrating the main injection site in the MD nucleus and the global extent of the corresponding antero-/retrograde thalamocortical projections. Tracing patterns are based on six animals. Very strong projections, full line; strong projections, hatched lines; dot, injection site. Scale bar = 1 cm.

a topographical description within MD of the thalamic projections from the anterior insular and the infralimbic area cannot be provided, because tracing from these areas were not successfully accomplished. No clear relationship with the frontal cortex could be established for the lateral densocellular area in the MD nucleus.

Cortical efferents were also demonstrated by in vivo tract tracing using manganese as an MRI-visible paramagnetic contrast agent (Fig. 8). Manganese turned out to be very sensitive with a dense labelling of main thalamic projection sites within a 2-day period. A good correlation was observed with the histological tracer when comparing the labelling of the MD nucleus (Fig. 8(K and L)). Similarly, the unilateral injections of manganese revealed high levels of corticocortical connectivity through the genu of the corpus callosum (Fig. 8(H and I)) as well as some degree of connections in the contralateral MD nucleus. Mn-MRI also revealed some of the segregated circuits that unite the frontal cortex, the thalamus and the basal ganglia (Fig. 8). A clear signal enhancement was observed in the pallidum (Fig. 8(B and C)) with further projections directed toward the thalamus or the substantia nigra/ventral brain tegmentum (Fig. 8(F and G)). Even though further nigrothalamic projections could not be detected, the in vivo tract tracing does indicate a transsynaptic transport of manganese.

### 3.3. Relative PFC volume

Volume estimates performed on thionine stained coronal sections revealed that the PFC constitutes a mean volume of 2.50 $cm^3$ (CV = 0.069, CE = 0.050). This is around 24% of the total isocortex volume (10.53 $cm^3$; CV = 0.077; CE = 0.044) and 10% of total brain volume (26.98 $cm^3$; CV = 0.13; CE = 0.054). When compared to fluid displacement volume of perfusion fixed whole brains we observe an almost 40% reduction in volume as a consequence of tissue processing. It is assumed that deformation in all regions equals the deformation in total brain volume.

## 4. Discussion

The distribution of reciprocal connections with the thalamic MD nucleus has been reported as a main criterion for the delineation of the PFC in a wide range of experimental

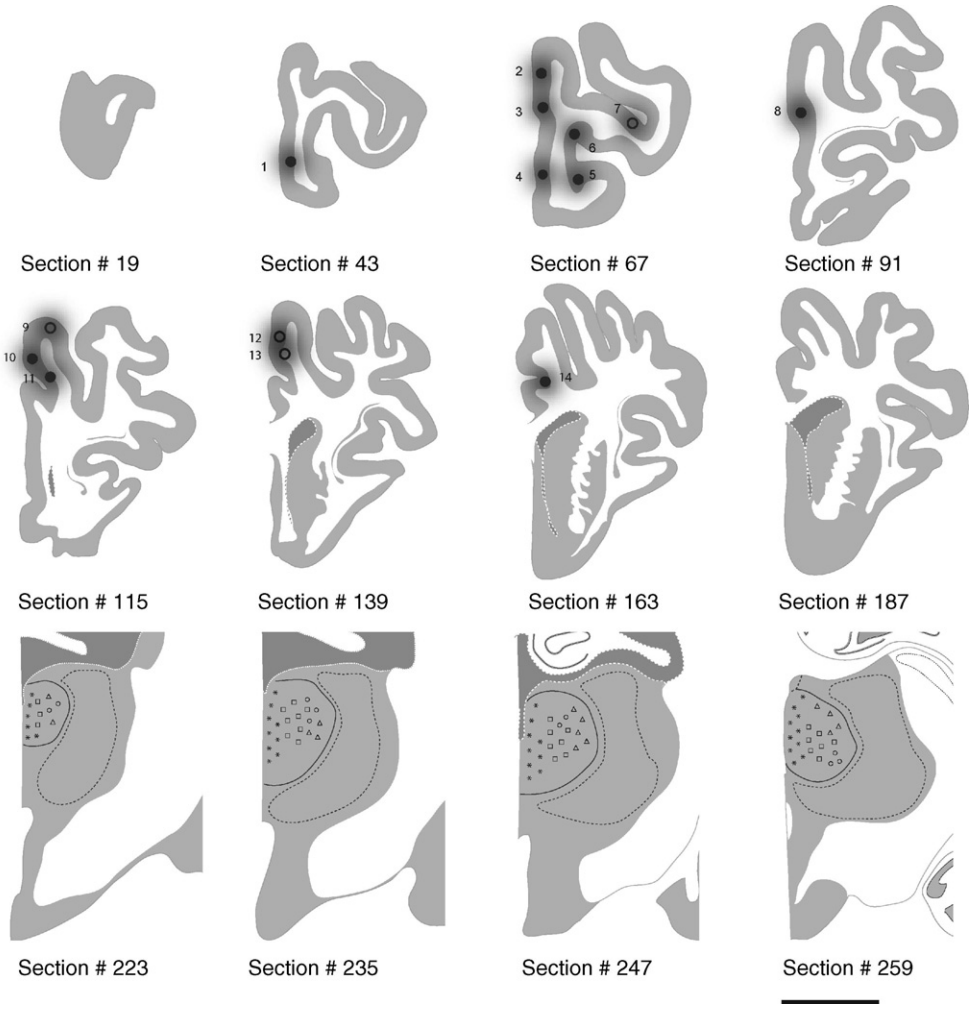


Fig. 7. Schematic illustration of coronal sections demonstrating all cortical injection sites and the corresponding antero-/retrograde corticothalamic projections. Cortical injections with strong connections to the MD nucleus are indicated with full circles. Cortical injections with strong connections to other thalamic nuclei are shown as empty circles. Five misplaced injections are not shown (Table 1). In the MD nucleus of the thalamus the following patterns are observed: asterisks; projection patterns related to the frontopolar injections (#1, 4–6). Squares; projections from rostral parts of the anterior cingulate (# 3, 8, 11). Triangles; projections from the more caudal parts of the anterior cingulate (#14). Circle; projections from the dorsofrontal PFC (#2, 10). Scale bar = 1 cm.

animals including non-human primates (e.g. [27]), sheep (e.g. [19]), dog (e.g. [60]), cat (e.g. [14,41]), Guinea pig (e.g. [40]), rabbit (e.g. [10]), rat (e.g. [29,36,65]) and mouse (e.g. [32]). The most important conclusion to be drawn from the present experiments in the young Göttingen minipig is that the MD nucleus also connects reciprocally to several distinct areas in the frontal lobe in this species. Furthermore, the MD nucleus in the young Göttingen minipig seems to be composed of separate compartments, which may be connected to different cytoarchitectonically defined areas in the PFC. Cytoarchitectonic and connectional data therefore strongly suggests that the PFC in the young Göttingen minipig is also structurally subdivided.

### *4.1. The PFC in the young Göttingen minipig*

Based on the presence of a granular layer IV and known as the "frontal granular cortex", the PFC was previously considered unique to the primate species [5]. The observation of a frontomedial area with a dysgranular layer IV in the pig brain [59] was therefore particularly noteworthy indicating possibly homology to the PFC of primates. However, even though a mediopolar frontal area was delineated in the present study we did not observe any granular or dysgranular layer IV in the Göttingen minipig. In fact, it turned out that the most characteristic feature of the Göttingen minipig frontal cortices was the complete absence of a cellular layer IV. The evaluation of thionin stained coronal sections revealed that the frontal lobe of the young Göttingen minipig can be differentiated into several cytoarchitectonically defined cortical areas with topographically organized connections with the MD nucleus. On this basis certain comparisons may be made with the PFC of other species, e.g. rat and primate.

#### *4.1.1. The frontopolar region*

The mediopolar frontal area in the young Göttingen minipig corresponds partly in position to the "orbitofrontal region" delineated in sheep and other animals [19,53]. This PFC region was originally restricted to the frontal pole and considered to be an

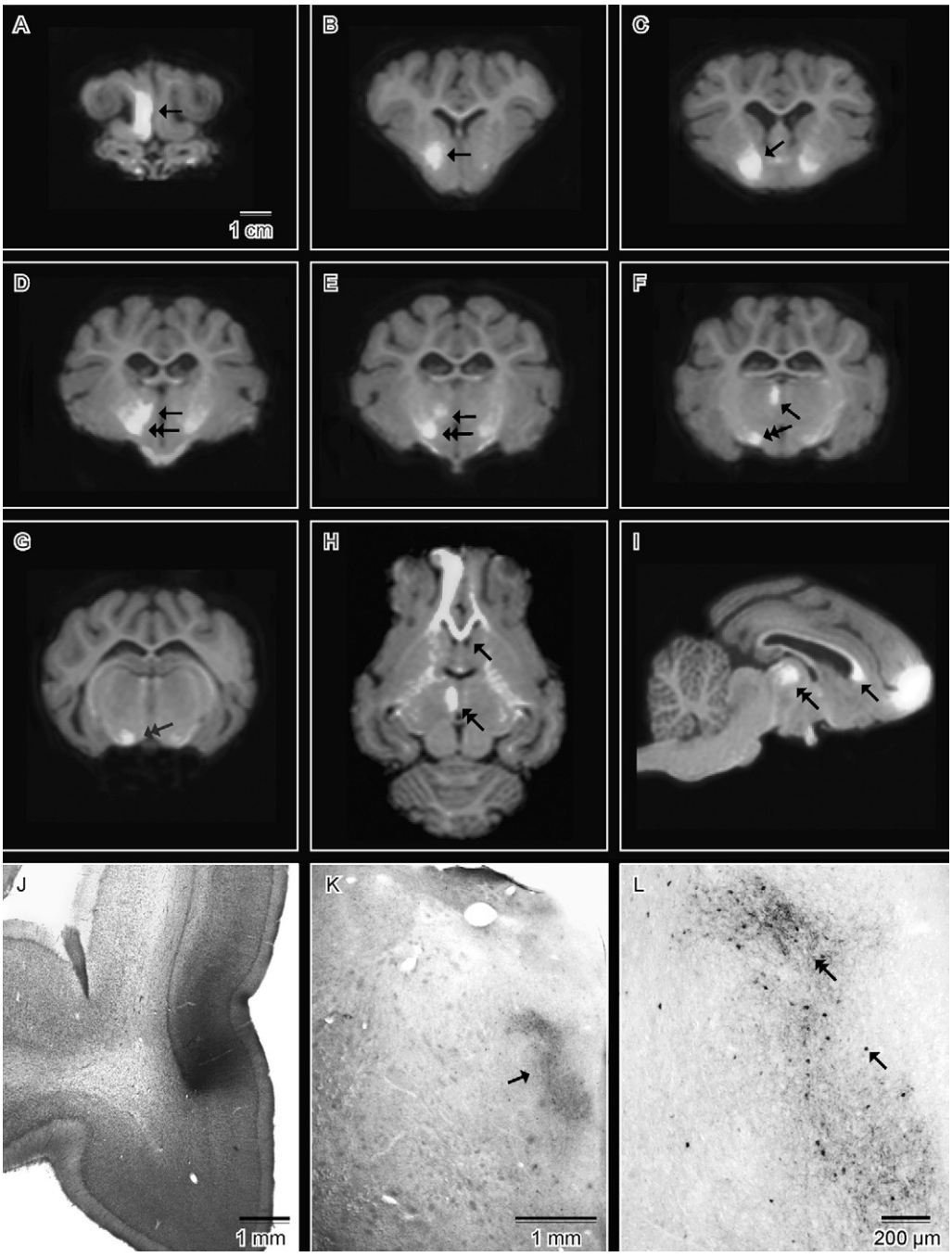


Fig. 8. MRI in vivo tract tracing, coronal section plane. (A) Manganese enhanced MRI of injection site (arrow) with labelling in vicinity of the globus pallidus (B, arrow) and the ventral pallidum (C, arrow). At this level, the tract is segregated into two major fibre bundles (D and E); one directed through the rostral part of the thalamus (E, arrow) towards the MD nucleus (F, arrow), and one directed ventrally toward the substantia nigra/ventral tegmentum (E–G, double arrow). (H and I) Corticocortical transport of tracer through the corpus callosum (arrow) with projections in the contralateral PFC (H, horizontal plane; I, sagittal plane). (J–L) Immunohistochemical visualization of simultaneously injected BDA, showing injection site (J) and projection site in medial MD nucleus (K, arrow). (L) Higher magnification of the retrogradely labelled BDA perikarya (arrow) and anterogradely labelled BDA terminal field (double arrow) in the thalamic MD nucleus.

equivalent to the PFC in primates [53], but the application of more sensitive tracing methods has made it obvious that the MD nucleus projects more widely within the frontal cortex (e.g. [63]). In the young Göttingen minipig the mpFr covers a substantial area of the frontal pole including ventral, lateral and medial cortices. It corresponds in position with the "granular frontal region" delineated by Stephan [59] and the "prefrontal area" briefly described by Campbell [11].

The thalamocortical connections to this frontopolar region originate mainly in the medial part of the MD nucleus. A similar organization of connections has been described for the medial PFC and the anterior orbital PFC of monkeys [13,28]. In rat, the orbital PFC connect mainly with the central part of the MD nucleus [29,36,50], but the pattern of orbital-MD connections in rat is in general rather complex and connections with the medial and lateral segment of the MD nucleus are also observed.

#### 4.1.2. The anterior cingulate region

Based on cytoarchitectonical and connectional differences, the cingulate cortex was divided into an anterior (AC) and posterior part (PC). However, the PC is not reciprocally connected with the MD nucleus and is hence not considered to be a part of the Göttingen minipig PFC. The AC was subdivided into a caudal inner and a rostrodorsal area, with a cytoarchitectonic resemblances to the primate area 24 and 32, respectively. The AC in the minipig seems to be strongly connected to the central and lateral part of the MD nucleus. The anterior cingulate cortex is also included in the primate and rat PFC with a topographical organization of connections mainly to the medial and lateral parts of the MD nucleus as well (e.g. [29,36,50,51,62,63]).

No injections were successfully positioned in the most caudal extensions of the AC, or in the infralimbic area of the minipig. It is still an open question whether the infralimbic area of the rat can be compared with the infralimbic area 25 in the primate. The rat IL belongs to the PFC (e.g. [36,62]), whereas area 25 has more reciprocal connections with thalamic ventral anterior nucleus [4,24]. Further research on this aspect is still required.

#### 4.1.3. The anterior insular region

The anterior insular region, located along the rhinal sulcus, was divided into a ventral (AIv), medial (AIm) and dorsal subdivision (AId). We exclude the latter from the PFC on basis of no clear connectivity with the MD nucleus. A similar organization can be distinguished in the monkey and rat cortex based on cytoarchitectonics and thalamic connections [42,50,51]. The macaque anterior insula is reciprocally connected with the MD nucleus, but these are not predominant and the anterior insula is consequently not considered to be a part of the primate PFC [63]. In contrary, the anterior insula is included in the rat PFC [29,36,62,63]. Our findings in the minipig brain indicate that the ventral and medial part of the anterior insula is strongly reciprocally connected with the MD nucleus and hence a component of the minipig PFC. However, as a consequence of unsuccessful tracer injections in the insular cortices, a specific origin from MD subnuclei could not be established. The possibility that the insular cortices connect more strongly with other thalamic nuclei, as in primates, can at present not be excluded.

#### 4.1.4. The dorsofrontal region

In contrast to Stephan [59] our analyses provides support for a division of the sigmoid and the superior frontal gyrus into three main dorsal frontal cortices; the dorsofrontal, the premotor and the primary motor cortex. From our tracing studies we conclude that the most rostral part of the superior frontal gyrus (i.e. the area 6 of Stephan [59]) has a more prefrontal than premotor-type of thalamic connection. Consequently, it is included into the pig PFC. It is divided into a dorsomedial and dorsolateral part. Both areas seem to be connected most strongly with the central and lateral part of the MD nucleus, but no cortical injections were restricted exclusively to the dlFr. In the monkey brain, the central parvocellular area of the MD nucleus connects mainly with the dorsomedial and dorsolateral prefrontal cortex [27,28] whereas the rat frontal area 2 (Fr2) or the precentral medial area, which is considered a dorsolateral-like PFC area (e.g. [62]), connects mainly with the lateral aspect of the MD nucleus. Despite some connectional similarity with the latter species and positional correspondence with the "shoulder cortex" in rat, more data is still needed to clarify whether the dorsofrontal PFC of the Göttingen minipig resembles the dorsolateral PFC of primates.

#### 4.1.5. Adjoining cortices

The region observed immediately caudal to the dorsofrontal PFC region (i.e. the area 4 by Stephan [59]) was here divided into a premotor-like area and a primary motor-like area. Both areas are not included in the minipig PFC. The M1 is positioned between the central ansate and the cruciate sulcus, i.e. in the sigmoid gyrus and corresponds in position to the motor cortex delineated from recordings of evoked potentials [7,45].

At the dorsolateral extreme, the dorsofrontal and the anterior insular region are bordered by a more or less homogeneous area, which has been considered analogous to the somatosensory cortex of other species (Brodmann area 2–3 by Stephan [59]). This interpretation is corroborated from evoked potential and microelectrode mapping (e.g. [3,15,16,69]). It also finds support from our single anterograde injection, demonstrating strong cortical connectivity with the ventral posterior and the ventral posterior lateral nucleus of the thalamus (Table 1). A similar projection pattern is generally recognised for somatosensory cortices [35].

### 4.2. Quantitative and developmental aspects

The PFC in the Göttingen minipig brain was found to occupy a considerable part of the frontal lobe. To make an approximate quantitative comparison with the PFC of rat and primate [63] we estimated the relative volume of PFC gray matter from five young Göttingen minipigs using the stereological Cavalieri principle [33]. The PFC makes up 24% of the total isocortex volume and 10% of the total brain volume in the minipig, which is comparable to the PFC ratio in rat, and rather close to the 25–30% observed in humans [63]. However, one has to realize that ratios are not appropriate for comparing quantitative information between species. Interspecies differences may be a consequence of allometric relation or segregation of cortical regions, and the relative PFC volume by itself cannot be considered an indication of its cognitive capability [63].

A study of the postnatal developmental of rat PFC reveals that the volume of especially medial and orbital parts of the PFC reach a significantly larger value during the first 30 days of postnatal life than in adulthood [66]. In the Göttingen minipig the total brain weight increases more than 2-fold from time of birth to 3 months of age. A transient overgrowth for the PFC in these young Göttingen minipigs cannot be excluded and may have an impact on the presented PFC ratios.

In contrary, we have no reason to doubt that MD-PFC reciprocal connections are not fully established in the young Göttingen minipig which we studied. The development of corresponding connections in the rat brain seems to be fully established already at postnatal Day 10 [65], and developmental data in the pig brain suggests that the main development in terms of myelination, composition and electrical activity has taken place within the first 8–10 weeks post partum [20,23,46,61].

### 4.3. Methodological considerations

The high variability in pig skull morphology, which is a consequence of the well-developed pneumatized frontal sinus, has previously led to a systematic use of ventriculography when defining the horizontal zero plane [39]. However, because the frontal sinus was less developed in the young Göttingen minipig and the variability in skull morphology using pigs of similar age and weight was expected to be low, the stereotaxic zero point and stereotaxic planes were here defined on external skull structures keeping the head in a relative fixed position using horizontal ear-bars and a mouth piece. However, the use of young Göttingen minipigs made it unfeasible to rely on available stereotaxic atlases of pig brains [22,56,67,70]. Furthermore, small variations in stereotaxic fixation and skull morphology led to difficulties in performing optimal injections in specific cortical subregions, e.g. the insular cortices. Recently, MRI compatible localizers have been developed which may facilitate future stereotaxic procedures in the pig brain [6,25].

To the present authors knowledge there have been no previous neuron tract tracing studies of reciprocal thalamocortical projections in the pig brain. Here we successfully applied the anterograde BDA and the retrograde ChB technique. In an attempt to refine our method and improve the assessment of tracings from the large pressure injection sites we tried to decrease the amount of injected tracer 10-fold, with a corresponding reduced and less sensitive labelling of the projection sites as a disadvantageous result. We then applied manganese, a paramagnetic in vivo MRI detectable tracer transported anterogradely along axons [47], which previously has been used to track axons in rodents [38] and used as indicator of neuronal connections of basal ganglia in monkeys [55]. Manganese created a clear signal enhancement on MR images making it possible to assess tracings from injection sites through white matter tracts to its final target. When compared to the simultaneously injected histological tracer, the correspondence between in vivo and histological labelling of thalamic projection sites was high.

The limited resolution and partial volume effects makes it difficult to unambiqously assess the deposition of manganese in the basal ganglia. However, the further labelling of the ventral brain nuclei does indicate that manganese may act as a transsynaptic tracer in accordance with in vivo tracings on, e.g. the striatopallidal system in the Macaque monkey [55]. The presented Mn-MRI tracings in the pig brain hereby support the existence of a PFC-basal ganglia-thalamocortical circuit comparable to that described in other animals (e.g., [1,2,31]). BDA, however, is not a transsynaptic tracer and is likely to be transported directly between cortex and thalamus following a pathway through the ventral and medial aspect of the internal capsule, as described from studies in the rat and monkey brain [17,29,34,36].

## 5. Conclusion

Using the distribution of reciprocal connections between the MD thalamic nucleus and the frontal lobe as a main criterion for the PFC, we provide a first map of the PFC in the young Göttingen minipig brain. The delineated PFC is rather large covering the rostral part of the superior frontal gyrus, the frontomedial cortex, the anterior cingulate as well as the anterior insular hidden within the deep rhinal sulcus (Fig. 1). However, several problems were encountered that influenced the refinement of the study, e.g. the precision of stereotaxic injections and the possible diffusion of pressure injected tracer. This should of course be taken into consideration in the evaluation and assessment of the presented result. Additional tracing studies are desirable for the topographic thalamic organisation of connections from the anterior insular- and the infralimbic area.

It should be emphasized, that the reciprocal connectivity of the frontal cortex with the MD nucleus does not provide strict criteria for defining the PFC. Even though it may be argued that the PFC must be considered as that part of the frontal lobe with the strongest reciprocal connections with the MD nucleus [63] it is, even with the use of modern tract tracing techniques, rather difficult to determine unequivocally which areas that receives the strongest connections. Realizing the pitfalls of our definition of the prefrontal cortex in the young Göttingen minipig, our study does provide a baseline for future more refined neural-tract tracing experiments and for further studies on other prefrontal anatomical and physiological characteristics.

## References

[1] G.E. Alexander, M.D. Crutcher, M.R. DeLong, Basal ganglia-thalamocortical circuits: parallel substrates for motor, oculomotor, "prefrontal" and "limbic" functions, Prog. Brain Res. 85 (1990) 119–146.
[2] G.E. Alexander, M.R. DeLong, P.L. Strick, Parallel organization of functionally segregated circuits linking basal ganglia and cortex, Annu. Rev. Neurosci. 9 (1986) 357–381.
[3] R.J. Andrews, R.T. Knight, R.P. Kirby, Evoked potential mapping of auditory and somatosensory cortices in the miniature swine, Neurosci. Lett. 114 (1990) 27–31.
[4] H. Barbas, H.T. Ghasghaei, N.L. Rempel-Clower, D. Xiao, Anatomic basis of functional specialization in prefrontal cortices in primate Handbook of Neuropsychology, vol. 7, Elsevier, Amsterdam, 2002, pp. 1–27.
[5] A.L. Benton, The prefrontal region: its early history, in: H.S. Levin, H.M. Eisenberg, A.L. Benton (Eds.), Frontal Lobe Function and Dysfunction, Oxford University Press, New York, 1991, pp. 3–32.
[6] C.R. Bjarkam, G. Cancian, M. Larsen, F. Rosendahl, K.S. Ettrup, D. Zeidler, A.D. Blankholm, L. Ostergaard, N. Sunde, J.C. Sorensen, A MRI-compatible stereotaxic localizer box enables high-precision stereotaxic procedures in pigs, J. Neurosci. Methods 139 (2004) 293–298.
[7] J.E. Breazile, B.C. Swafford, W.D. Thomson, Study of the motor cortex of the domestic pig, Am. J. Vet. Res. 27 (1966) 1369–1373.
[8] K. Brodmann, Vergleichence Lokalisationslehre der Grosshirnhinde, Barth, Leipzig, 1909.
[9] K. Brodmann, Neue ergebnisse über die vergleichende histologische lokalisation der grosshirnrinde mit besonderer berücksichtigung des stirnhirns, Anat. Anz. 21 (1912) 157–216.
[10] S.L. Buchanan, D.A. Powell, R.H. Thompson, Prefrontal projections to the medial nuclei of the dorsal thalamus in the rabbit, Neurosci. Lett. 106 (1989) 55–59.
[11] A.W. Campbell, Histological Studies on The Localisation of Cerebral Function, Cambridge University Press, Cambridge, 1905.
[12] C.B. Campbell, W. Hodos, The concept of homology and the evolution of the nervous system, Brain Behav. Evol. 3 (1970) 353–367.
[13] C. Cavada, F. Reinoso-Suarez, Topographical organization of the cortical afferent connections of the prefrontal cortex in the cat, J. Comp. Neurol. 242 (1985) 293–324.

[14] C. Cavada, T. Company, J. Tejedor, R.J. Cruz-Rizzolo, F. Reinoso-Suarez, The anatomical connections of the macaque monkey orbitofrontal cortex. A review, Cereb. Cortex. 10 (2000) 220–242.
[15] S.L. Craner, R.H. Ray, Somatosensory cortex of the neonatal pig: I. Topographic organization of the primary somatosensory cortex (SI), J. Comp. Neurol. 306 (1991) 24–38.
[16] S.L. Craner, R.H. Ray, Somatosensory cortex of the neonatal pig: II. Topographic organization of the secondary somatosensory cortex (SII), J. Comp. Neurol. 306 (1991) 39–48.
[17] J.L. DeVito, M.E. Anderson, An autoradiographic study of efferent connections of the globus pallidus in Macaca mulatta, Exp. Brain Res. 46 (1982) 107–117.
[18] J.W.T. Dickerson, J. Dobbing, Prenatal and postnatal growth and development of the central nervous system of the pig, Proc. R. Soc. Med. 166 (1966) 384–395, series B.
[19] A. Dinopoulos, A.N. Karamanlidis, G. Papadopoulos, J. Antonopoulos, H. Michaloudi, Thalamic projections to motor, prefrontal, and somatosensory cortex in the sheep studied by means of the horseradish peroxidase retrograde transport method, J. Comp. Neurol. 241 (1985) 63–81.
[20] M. Fang, J. Li, X. Gong, G. Antonio, F. Lee, W.H. Kwong, S.M. Wai, D.T. Yew, Myelination of the pig's brain: a correlated MRI and histological study, Neurosignals 14 (2005) 102–108.
[21] M. Fang, J. Li, J.A. Rudd, S.M. Wai, J.C. Yew, D.T. Yew, fMRI Mapping of cortical centers following visual stimulation in postnatal pigs of different ages, Life Sci. (2005) [Epub ahead of print].
[22] B. Felix, M.E. Leger, D. Albe-Fessard, J.C. Marcilloux, O. Rampin, J.P. Laplace, Stereotaxic atlas of the pig brain, Brain Res. Bull. 49 (1999) 1–137.
[23] T.J. Flynn, Developmental changes of myelin-related lipids in brain of miniature swine, Neurochem. Res. 9 (1984) 935–945.
[24] L.J. Freedman, T.R. Insel, Y. Smith, Subcortical projections of area 25 (subgenual cortex) of the macaque monkey, J. Comp. Neurol. 421 (2000) 172–188.
[25] S. Frey, R. Comeau, B. Hynes, S. Mackey, M. Petrides, Frameless stereotaxy in the nonhuman primate, Neuroimage 23 (2004) 1226–1234.
[26] J.M. Fuster, The Prefrontal Cortex: Anatomy, Physiology and Neuropsychology of the Frontal Lobe, Lippincott-Raven, Philadelphia, 1997.
[27] M. Giguere, P.S. Goldman-Rakic, Mediodorsal nucleus: areal, laminar, and tangential distribution of afferents and efferents in the frontal lobe of rhesus monkeys, J. Comp. Neurol. 277 (1988) 195–213.
[28] P.S. Goldman-Rakic, L.J. Porrino, The primate mediodorsal (MD) nucleus and its projection to the frontal lobe, J. Comp. Neurol. 242 (1985) 535–560.
[29] H.J. Groenewegen, Organization of the afferent connections of the mediodorsal thalamic nucleus in the rat, related to the mediodorsal-prefrontal topography, Neuroscience 24 (1988) 379–431.
[30] H.J. Groenewegen, M.P. Witter, Thalamus, in: G. Paxinos (Ed.), The Rat Nervous System, third ed., Academic Press, San Diego, CA, 2004, pp. 407–453.
[31] H.J. Groenewegen, C.I. Wright, H.B.M. Uylings, The anatomical relationships of the prefrontal cortex with limbic structures and the basal ganglia, J. Psychopharmacol. 11 (1997) 99–106.
[32] W.O. Guldin, M. Pritzel, H.J. Markowitsch, Prefrontal cortex of the mouse defined as cortical projection area of the thalamic mediodorsal nucleus, Brain Behav. Evol. 19 (1981) 93–107.
[33] H.J. Gundersen, E.B. Jensen, The efficiency of systematic sampling in stereology and its prediction, J. Microsc. 147 (1987) 229–263.
[34] S.N. Haber, K. Kunishio, M. Mizobuchi, E. Lynd-Balta, The orbital and medial prefrontal circuit through the primate basal ganglia, J. Neurosci. 15 (1995) 4851–4867.
[35] E.G. Jones, The Thalamus, Plenum Press, New York, 1985.
[36] J.E. Krettek, J.L. Price, The cortical projections of the mediodorsal nucleus and adjacent thalamic nuclei in the rat, J. Comp. Neurol. 171 (1977) 157–191.
[37] D. Kruska D, Volumenvergleich optischer Hirnzentren bei Wild- und Hausschweinen, Z. Anat. Entwicklungsgesch 138 (1972) 265–282.
[38] T.B. Leergaard, J.G. Bjaalie, A. Devor, L.L. Wald, A.M. Dale, In vivo tracing of major rat brain pathways using manganese-enhanced magnetic resonance imaging and three-dimensional digital atlasing, Neuroimage 20 (2003) 1591–1600.
[39] J.C. Marcilloux, O. Rampin, M.B. Felix, J.P. Laplace, D. Albe-Fessard, A stereotaxic apparatus for the study of the central nervous structures in the pig, Brain Res. Bull. 22 (1989) 591–607.
[40] H.J. Markowitsch, M. Pritzel, Prefrontal cortex of the guinea pig (*Cavia porcellus*) defined as cortical projection area of the thalamic mediodorsal nucleus, Brain Behav. Evol. 18 (1981) 80–95.
[41] H.J. Markowitsch, M. Pritzel, I. Divac, The prefrontal cortex of the cat: anatomical subdivisions based on retrograde labeling of cells in the mediodorsal thalamic nucleus, Exp. Brain Res. 32 (1978) 335–344.
[42] M.M. Mesulam, E.J. Mufson, Insula of the old world monkey I. Architectonics in the insulo-orbito-temporal component of the paralimbic brain, J. Comp. Neurol. 212 (1982) 1–22.
[43] MIPAV ref.: http://mipav.cit.nih.gov/.
[44] Y. Okada, A. Lahteenmaki, C. Xu, Comparison of MEG and EEG on the basis of somatic evoked responses elicited by stimulation of the snout in the juvenile swine, Clin. Neurophysiol. 110 (1999) 214–229.
[45] G. Palmieri, V. Farina, R. Panu, A. Asole, L. Sanna, P.L. de Riu, C. Gabbi, Course and termination of the pyramidal tract in the pig, Arch. Anat. Microsc. 75 (1987) 167–176.
[46] G. Pampiglione, Some aspects of development of cerebral function in mammals, Proc. R. Soc. Med. 64 (1971) 429–435.
[47] R.G. Pautler, A.C. Silva, A.P. Koretsky, In vivo neuronal tract tracing using manganese-enhanced magnetic resonance imaging, Magn. Reson. Med. 40 (1998) 740–748.
[48] D. Plogmann, D. Kruska, Volumetric comparison of auditory structures in the brains of European wild boars (*Sus scrofa*) and domestic pigs (*Sus scrofa f. dom*), Brain Behav. Evol. 35 (1990) 146–155.
[49] T.M. Preuss, Do rats have a prefrontal cortex? The Rose–Woolsey–Akert program reconsidered, J. Cogn. Neurosci. 7 (1995) 1–24.
[50] J.P. Ray, J.L. Price, The organization of the thalamocortical connections of the mediodorsal thalamic nucleus in the rat, related to the ventral forebrain-prefrontal cortex topography, J. Comp. Neurol. 323 (1992) 167–197.
[51] J.P. Ray, J.L. Price, The organization of projections from the mediodorsal nucleus of the thalamus to orbital and medial prefrontal cortex in macaque monkeys, J. Comp. Neurol. 337 (1993) 1–31.
[52] J.E. Rose, The thalamus of the sheep: cellular and fibrous structure and comparison with pig, rabbit and cat, J. Comp. Neurol. 77 (1942) 469–523.
[53] J.E. Rose, C.N. Woolsey, The orbitofrontal cortex and its connections with the mediodorsal nucleus in rabbit, sheep and cat, Res. Publ. Assoc. Nerv. Ment. Dis. 27 (1948) 210–232.
[54] T. Saito, C.R. Bjarkam, M. Nakamura, T. Nemoto, Determination of stereotaxic coordinates for the hippocampus in the domestic pig, J. Neurosci. Methods 80 (1998) 29–36.
[55] K.S. Saleem, J.M. Pauls, M. Augath, T. Trinath, B.A. Prause, T. Hashikawa, N.K. Logothetis, Magnetic resonance imaging of neuronal connections in the macaque monkey, Neuron 34 (2002) 685–700.
[56] M.E. Salinas-Zeballos, G.A. Zeballos, P.M. Gootman, A stereotaxic atlas of the developing swine (*Sus scrofa*) forebrain, in: M.E. Tumbleson (Ed.), Swine in Biomedical Research, vol. 2, Plenum Publishers, New York, 1986, pp. 887–906.
[57] O. Solnitzky, The thalamic nuclei of *Sus scrofa*, J. Comp. Neurol. 69 (1938) 121–169.
[58] SPM2: http://www.fil.ion.ucl.ac.uk/spm/software/.
[59] H. Stephan, Vergleichende Untersuchungen über Feinbau des Hirnes von Wild- und Haustieren, Zool. Jahrb. Abt. Anat. Ontog. Tiere. 71 (1951) 487–586.
[60] I. Stepniewska, A. Kosmal, Distribution of mediodorsal thalamic nucleus afferents originating in the prefrontal association cortex of the dog, Acta Neurobiol. Exp. 46 (1986) 311–322.
[61] K.L. Thibault, S.S. Margulies, Age-dependent material properties of the porcine cerebrum: effect on pediatric inertial head injury criteria, J. Biomech. 31 (1998) 1119–1126.
[62] H.B.M. Uylings, H.J. Groenewegen, B. Kolb, Do rats have a prefrontal cortex? Behav. Brain Res. 146 (2003) 3–17.

[63] H.B.M. Uylings, C.B. van Eden, Qualitative and quantitative comparison of the prefrontal cortex in rat and in primates, including humans, Prog. Brain Res. 85 (1990) 31–62.
[64] Y.D. Van der Werf, M.P. Witter, H.J. Groenewegen, The intralaminar and midline nuclei of the thalamus. Anatomical and functional evidence for participation in processes of arousal and awareness, Brain Res. Rev. 39 (2002) 107–140.
[65] C.G. Van Eden, Development of connections between the mediodorsal nucleus of the thalamus and the prefrontal cortex in the rat, J. Comp. Neurol. 244 (1986) 349–359.
[66] C.G. Van Eden, H.B.M. Uylings, Postnatal volumetric development of the prefrontal cortex in the rat, J. Comp. Neurol. 241 (1985) 268–274.
[67] H. Watanabe, F. Andersen, C.Z. Simonsen, S.M. Evans, A. Gjedde, P. Cumming, MR-based statistical atlas of the Gottingen minipig brain, Neuroimage 14 (2001) 1089–1096.
[68] S.A. Weaver, A.L. Schaefer, W.T. Dixon, Western blotting for detection of glucocorticoid receptors in the brain and pituitary gland from adrenal intact pigs, Brain Res. 869 (2000) 130–136.
[69] C.N. Woolsey, M.D. Fairman, Contralateral, ipsilateral, and bilateral representation of cutaneous receptors in somatic areas I and II of the cerebral cortex of pig, sheep, and other mammals, Surgery 19 (1946) 684–702.
[70] T. Yoshikawa, The brain of the pig, in: The Atlas of the Brains of Domestic Animals, University of Tokyo Press, Tokyo, 1968.